Check for updates

Received: 16 April 2021 | Revised: 14 June 2021 | Accepted: 8 July 2021

DOI: 10.1002/aoc.6383

Applied Organometallic Chemistry WILEY

RESEARCH ARTICLE

Amine-functionalized nano-NaY zeolite for the synthesis of *N*-acetyl pyrazoles and dihydropyrimidines

Raheleh Razavian Mofrad[1] | **Hassan Kabirifard**[1] | **Mahmood Tajbakhsh**[2] | **Ghasem Firouzzadeh Pasha**[2]

[1]Department of Chemistry, Islamic Azad University, Tehran North Branch, Tehran, Iran

[2]Department of Organic Chemistry, Faculty of Chemistry, University of Mazandaran, Babolsar, Iran

Correspondence
Mahmood Tajbakhsh, Department of Organic Chemistry, Faculty of Chemistry, University of Mazandaran, Babolsar 47416-95447, Iran.
Email: tajbaksh@umz.ac.ir

Funding information
Islamic Azad University, Tehran North Branch; University of Mazandaran

An efficient base-catalyzed synthesis of dihydropyrimidines and *N*-acetyl pyrazoles is reported using 1-(2-aminoethyl)piperazine-modified nano-NaY zeolite (ZeSi–AP) under mild and green conditions. The structure of the catalyst was identified by using FT-IR, XRD, TGA, DTA, DLS, SEM, TEM, and elemental analyses. This heterogeneous catalyst has many benefits, such as a simple work-up procedure, high product yield, and it is easily regenerated and reused at least for four cycles without losing its activity.

KEYWORDS
amine functionalized, dihydropyrimidines, green chemistry, *N*-acetyl pyrazoles, NaY zeolite

1 | INTRODUCTION

The application of solid catalysts in organic reactions is an important issue to achieve green and efficient catalysts, as they are widely used in environmentally friendly chemical processes.[1] Recently, many homogeneous catalysts were supported on the inorganic materials to overcome the disadvantage of homogeneous catalysts such as difficulty of catalyst separation, using distillation and extraction procedures, and reusability of catalyst.[2] One example of inorganic supporting materials is nanozeolites due to their thermal stability, availability, nontoxicity, nanosized and large surface-to-volume ratio, and reusability.[3] Functionalization of nanozeolites with organic molecules has found many interests during last decades.[4] For example, amine-functionalized nanozeolites have been used as catalyst in organic transformations and also as efficient sorbents for capturing of gases such as CO_2, H_2S, and methane from gas streams.[5]

N-Heterocyclic compounds including dihydropyrimidines (DHPMs),[6a] pyrroles,[6b] imidazoles,[6c] benzimidazoles,[6d] pyridines,[6e] pyrazines,[6f] and indoles[6f] have a vital role in chemistry because of their pharmaceutical activities. DHPMs are considered as essential biological active compounds due to their activities as anti-inflammatory agents,[7a] antihypertensive,[7b] anti-HIV,[7c] antitumor,[7d] calcium channel blockers,[7e] and antibacterial.[7f] In addition, many natural compounds containing dihydropyrimidine moiety in their structures exhibit fascinating pharmaceutical properties.[8]

The Biginelli reaction for the preparation of DHPMs involves condensation of beta-keto esters, urea, and aldehydes in acidic media.[9a] The major disadvantage of this protocol is the substrate tolerance and low yields of products.[9b]

Several catalysts that reported for the synthesis of DHPMs include $InBr_3$,[10a] $InCl_3$,[10b] $LiClO_4$,[10c] $FeCl_3{\cdot}6H_2O$,[10d] $NiCl_2{\cdot}6H_2O$,[10e] $CuCl_2$,[10f] $LaCl_3{\cdot}7H_2O$,[10g] bismuth triflate,[10h] $BF_3{\cdot}$EtOH/copper (II) chloride,[10i] and boric acid.[10j]

Besides, five-membered heterocyclic rings possessing two nitrogen atoms named as pyrazoles are known as biological active molecules and important precursors for the preparation of pyrazoline derivatives including cyanopyridine, indoxacarb, carbohydrazide hydrazine,

 © 2021 John Wiley & Sons, Ltd.

pyrimidine, and *N*-acetylated pyrazolines.[11] These heterocycles display various pharmaceutical properties such as treatment of Alzheimer's disease, anticancer, anti-allergic, and anti-inflammatory activities.[12] Several acidic and basic catalysts were reported to catalyze the synthesis of *N*-acetylated 4, 5-dihydro-1*H*-pyrazoles. These are included fly ash H_2SO_4,[11b] SiO_2Cl, triflouroacetic acid (TFA), methanesulfonic acid, 1,5,7-triazabicyclo[4.4.0]dec-5-ene (TBD), NaOH, Cs_2CO_3, and K_2CO_3.[13] Bauer et al. have synthesized *N*-acetylated pyrazolines in the presence of polymer bound bases.[14] Although there are many reports for the preparation of *N*-acetylated 4,5-dihydro-1*H*-pyrazole derivatives using various catalysts, the literature survey reveals that there is no information available for the preparation of these compounds in the presence of modified heterogeneous nanocatalysts. Although some of these methods resulted in high yield of DHPMs and pyrazole derivatives, many of these procedures suffer from disadvantages like expensive catalysts, long reaction time, low yields, strong acidic media, harsh reaction conditions, and difficult separation, recovery, and reusability of the catalyst. Hence, affords to find milder and more efficient procedure to synthesis DHPMs and pyrazole derivatives continued to attract many interests.

In this study, the synthesis of 1-(2-aminoethyl) pipirazine-functionalized NaY zeolite and its application as a heterogeneous catalyst in the preparation of dihydropyrimidin-2(1*H*)-ones and *N*-acetylated 4,5-dihydro-1*H*-pyrazole derivatives in green solvents is reported (Scheme 1).

2 | EXPERIMENTAL

2.1 | Methods and materials

3-Chloropropyl trimethoxysilane (CPTMS), 1-(2-amino ethyl)pipirazine (AP), triethylamine, and solvents were obtained from Merck company (Germany). NaY nanozeolite (Si/Al = 2.5) was provided from Zeolyst corporation (USA). The Electrothermal IA9100 (Essex, UK) was used to measure melting points. ^{1}H and ^{13}C NMR spectra were recorded by a Bruker Avance DRX-400 spectrometer (Bruker, Germany) using TMS as internal reference and in $CDCl_3$ and DMSO-d_6 as solvents. The synthesized catalyst was characterized by TGA apparatus (Netzsch, Selb, Germany), X-ray powder diffraction at room temperature using Cu Kα source (Philips PW-1830), FT-IR spectrometer (Bruker Tensor 27, Germany), scanning electron microscopy (SEM) on MIRA 3- XMU (Tescan, Brno, Czech Republic), dynamic light scattering (DLS) on HORIBA SZ-100 (HORIBA, Ltd., Japan), Brunauer–Emmett–Teller (BET) model, and t-plot (BELsorp, Japan).

2.2 | General procedure for the synthesis of amine-modified nanozeolites with 1-(2-aminoethyl)piperazine (ZeSi–AP)

NaY nanozeolite (Ze, 1 g) was added to anhydrous toluene and refluxed for 30 min under nitrogen atmosphere. Then, 3-cloropropyltrimethoxysilane (CPTMS, 1.82 ml, 10 mmol) was added into the above solution and refluxed for 4 h. The mixture was then cooled to room temperature and filtered off to collect the solid. The solid was extracted by a Soxhlet extractor using 150-ml ethanol (99.5%) for 24 h to remove the unreacted CPTMS.

After extraction, the solid was added to anhydrous dichloromethane (30 ml) and stirred at room temperature for 30 min under nitrogen. Then, 1-(2-aminoethyl) piperazine (AP) (1.31 ml, 10 mmol) and triethylamine (1.38 ml, 10 mmol) were mixed with the above mixture and stirred for 24 h at room temperature under inert atmosphere. The mixture was filtered off to collect the solid product ZeSi–AP, which then extracted by ethanol

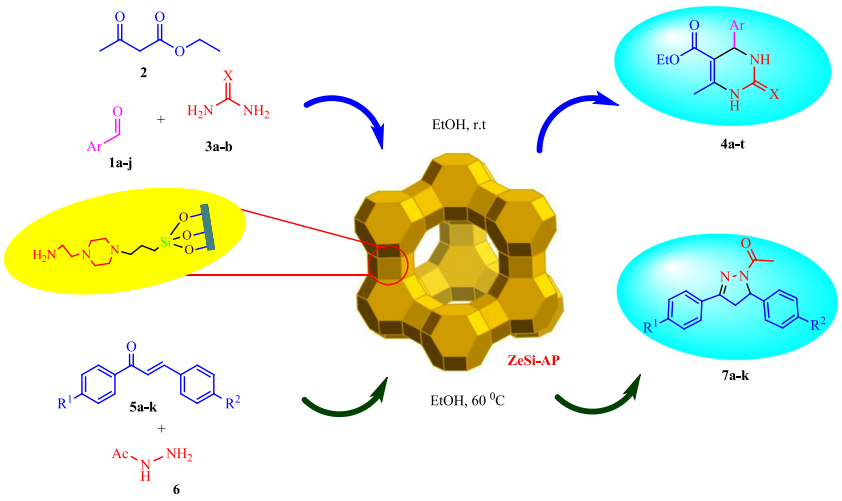

SCHEME 1 Synthesis of DHPMs and *N*-acetylated 4, 5-dihydro-1*H*-pyrazoles using functionalized NaY nanozeolite

(99.5%, 150 ml) in a Soxhlet extractor for 24 h to remove nongrafted amine. The solid product ZeSi–AP was dried in an oven for overnight.

2.3 | General procedure to prepare DHPMs 4a–n

Aldehyde (2 mmol), ethyl acetoacetate (2 mmol), either urea or thiourea (2.5 mmol), and ZeSi–AP (20 mg) in EtOH (10 ml) were mixed and stirred at room temperature for an appropriate time (Table 5). The mixture was filtered off and washed with ethanol to collect the catalyst. The filtrate was evaporated under vacuum to give the crude product, which then crystallized with ethanol to obtain the pure DHPM product. ^{1}H and ^{13}C NMR spectral data can be seen in Figures S1–S27.

2.4 | General procedure to prepare *N*-acetyl-substituted pyrazole derivatives 7a–n

Chalcone **1** (2 mmol), acylhydrazine **2** (2.4 mmol), and ZeSi–AP (25 mg) in EtOH (10 ml) were mixed and stirred at 60°C for an appropriate time (Table 8). Completion of reaction was controlled by thin-layer chromatography (TLC) using hexane/EtOAc (3:1) as eluent. The mixture was filtered off and washed with ethanol to collect the catalyst. The filtrate was evaporated under vacuum to leave a solid residue, which then recrystallized from ethanol to produce pure products **7a–n**. ^{1}H and ^{13}C NMR spectral data can be seen in Figures S28–S57.

2.5 | Spectral data for selected products

2.5.1 | Ethyl 4-(phenyl)-6-methyl-2-oxo-1,2,3,4-tetrahydropyrimidine-5-carboxylate (**4a**)

White powder; ^{1}H NMR ($CDCl_3$, 400 MHz): δ 1.18 (t, 3H, $^{3}J = 6.8$ Hz, CH_3), 2.36 (s, 3H, CH_3), 4.09 (q, 2H, $^{3}J = 6.8$ Hz, CH_2), 5.41 (s, 1H, CH), 5.73 (s, 1H, NH), 7.29–7.34 (m, 5H, $5CH_{Ar}$), 8.05 (s, 1H, NH); ^{13}C NMR ($CDCl_3$, 100 MHz): δ 165.4, 153.2, 146.4, 142.1, 133.7, 128.8, 128.0, 101.1, 60.1, 55.1, 18.7, 14.1.

2.5.2 | Ethyl4-(4-methoxyphenyl)-6-methyl-2-oxo-1,2,3,4-tetrahydropyrimidine-5-carboxylate (**4b**)

White powder; ^{1}H NMR (DMSO, 400 MHz): δ 1.10 (t, 3H, $^{3}J = 7.2$ Hz, CH_3), 2.24 (s, 3H, CH_3), 3.72 (s, 3H, OCH_3), 3.97 (q, 2H, $^{3}J = 7.2$ Hz, CH_2), 5.09 (d, 1H, $^{3}J = 2.8$ Hz, CH), 6.87 (d, 2H, $^{3}J = 8.8$, $2CH_{Ar}$), 7.14 (d, 2H, $^{3}J = 8.8$ Hz, $2CH_{Ar}$), 7.67 (s, 1H, NH), 9.15 (s, 1H, NH); ^{13}C NMR (DMSO, 100 MHz): δ 165.8, 158.9, 152.6, 148.4, 137.5, 127.8, 114.1, 100.0, 59.6, 55.5, 53.7, 18.2, 14.5.

2.5.3 | Ethyl 4-(3-hydroxyphenyl)-6-methyl-2-oxo-1,2,3,4-tetrahydropyrimidine-5-carboxylate (**4c**)

White powder; ^{1}H NMR (DMSO, 400 MHz): δ 1.10 (t, 3H, $^{3}J = 7.2$ Hz, CH_3), 2.24 (s, 3H, CH_3), 3.97 (q, 2H, $^{3}J = 8.4$ Hz, CH_2), 5.42 (s, 1H, CH), 6.64–6.61 (m, 3H, $2CH_{Ar}$ + NH), 6.74 (d, 2H, $^{3}J = 7.2$, CH_{Ar}), 8.65 (s, 1H, OH), 9.36 (s, 1H, NH); ^{13}C NMR (DMSO, 100 MHz): δ 167.7, 158.0, 157.6, 150.6, 144.5, 129.5, 116.9, 114.3, 113.4, 101.0, 59.4, 52.9, 18.1, 14.5.

2.5.4 | Ethyl 4-(2-hydroxyphenyl)-6-methyl-2-oxo-1,2,3,4-tetrahydropyrimidine-5-carboxylate (**4d**)

White powder; ^{1}H NMR (DMSO, 400 MHz): δ 0.99 (t, 3H, $^{3}J = 7.2$ Hz, CH_3), 2.23 (s, 3H, CH_3), 3.89 (q, 2H, $^{3}J = 8.4$ Hz, CH_2), 5.71 (s, 1H, CH), 7.02 (d, 2H, $^{3}J = 8.0$, CH_{Ar}), 7.5–7.54 (td, 2H, $^{3}J = 8.0$, $^{4}J = 1.6$, $2CH_A$), 7.66 (dd, 2H, $^{3}J = 8.0$, $^{4}J = 1.6$, CH_{Ar}), 7.71 (s, 1H, NH), 9.33 (s, 1H, OH), 10.26 (s, 1H, NH); ^{13}C NMR (DMSO, 100 MHz): δ 167.7, 158.0, 157.6, 150.6, 144.5, 129.5, 116.9, 114.3, 113.4, 101.0, 59.4, 52.9, 18.1, 14.5.

2.5.5 | Ethyl 4-(4-chlorophenyl)-6-methyl-2-oxo-1,2,3,4-tetrahydropyrimidine-5-carboxylate (**4e**)

White powder; ^{1}H NMR ($CDCl_3$, 400 MHz): δ 1.18 (t, 3H, $^{3}J = 7.2$ Hz, CH_3), 2.36 (s, 3H, CH_3), 4.09 (q, 2H, $^{3}J = 7.2$ Hz, CH_2), 5.39 (s, 1H, CH), 5.91 (s, 1H, NH), 7.27 (d, 2H, $^{3}J = 8.4$ Hz, 2H, $2CH_{Ar}$), 7.29 (d, 2H, $^{3}J = 8.4$ Hz, 2H, $2CH_{Ar}$), 8.18 (s, 1H, NH); ^{13}C NMR ($CDCl_3$, 100 MHz): δ 165.6, 153.2, 146.2, 143.6, 128.7, 127.9, 126.4, 101.4, 60.0, 65.1, 55.8, 18.7, 14.1.

2.5.6 | Ethyl 4-(2-chlorophenyl)-6-methyl-2-oxo-1,2,3,4-tetrahydropyrimidine-5-carboxylate (**4f**)

White powder; ^{1}H NMR (DMSO, 400 MHz): δ 0.99 (t, 3H, $^{3}J = 7.2$ Hz, CH_3), 2.30 (s, 3H, CH_3), 3.89 (q, 2H,

$^3J = 7.2$ Hz, CH_2), 5.42 (s, 1H, CH), 7.32–7.30 (m, 3H, $3CH_{Ar}$), 7.40 (d, 1H, $^3J = 7.6$ Hz, CH_{Ar}), 7.70 (s, 1H, NH), 9.27 (s, 1H, NH); ^{13}C NMR (DMSO, 100 MHz): δ 165.4, 157.7, 151.7, 149.7, 142.1, 132.1, 129.8, 128.2, 98.3, 57.7, 51.9, 18.1, 14.3.

2.5.7 | Ethyl 4-(2,4-dichlorophenyl)-6-methyl-2-oxo-1,2,3,4-tetrahydropyrimidine-5-carboxylate (**4g**)

White powder; ^{1}H NMR (DMSO, 400 MHz): δ 1.00 (t, 3H, $^3J = 7.2$ Hz, CH_3), 2.29 (s, 3H, CH_3), 3.89 (q, 2H, $^3J = 7.2$ Hz, CH_2), 5.59 (s, 1H, CH), 7.31 (d, 1H, $^3J = 8.4$ Hz, CH_{Ar}), 7.41 (dd, 1H, $^3J = 8.4$ Hz and $^4J = 2.0$ Hz, CH_{Ar}), 7.56 (d, 1H, $^4J = 2.4$ Hz, CH_{Ar}), 7.74 (s, 1H, NH), 9.30 (s, 1H, NH); ^{13}C NMR (DMSO, 100 MHz): δ 165.2, 151.6, 150.0, 141.4, 133.1, 133.0, 129.1, 128.4, 97.9, 59.6, 51.6, 18.1, 14.3.

2.5.8 | Ethyl 4-(4-cyanophenyl)-6-methyl-2-oxo-1,2,3,4-tetrahydropyrimidine-5-carboxylate (**4h**)

White powder; ^{1}H NMR (DMSO, 400 MHz): δ 1.08 (t, 3H, $^3J = 7.2$ Hz, CH_3), 2.25 (s, 3H, CH_3), 3.97 (q, 2H, $^3J = 7.2$ Hz, CH_2), 5.21 (d, 1H, $^3J = 2.0$ Hz, CH), 7.42 (d, 2H, $^3J = 8.0$, CH_{Ar}), 7.81 (d, 2H, $^3J = 8.4$ Hz, CH_{Ar}), 7.58 (s, 1H, NH), 9.31 (s, 1H, NH); ^{13}C NMR (DMSO, 100 MHz): δ 165.5, 152.2, 150.4, 149.7, 133.0, 127.8, 119.2, 110.5, 98.7, 59.8, 51.6, 18.2, 14.5.

2.5.9 | Ethyl 4-(4-nitrophenyl)-6-methyl-2-oxo-1,2,3,4-tetrahydropyrimidine-5-carboxylate (**4i**)

White powder; ^{1}H NMR ($CDCl_3$, 400 MHz): δ 1.21 (t, 3H, $^3J = 6.8$ Hz, CH_3), 2.38 (s, 3H, CH_3), 4.12 (q, 2H, $^3J = 6.8$ Hz, CH_2), 5.54 (s, 1H, CH), 5.82 (s, 1H, NH), 7.54 (d, 2H, $^3J = 7.6$ Hz, 2H, $2CH_{Ar}$), 7.67 (s, 1H, NH), 8.20 (d, 2H, $^3J = 7.6$ Hz, 2H, $2CH_{Ar}$); ^{13}C NMR ($CDCl_3$, 100 MHz): δ 165.1, 150.3, 147.5, 144.6, 127.6, 123.9, 100.59, 96.6, 60.4, 55.1, 18.7, 14.2.

2.5.10 | 1-Acetyl-3-(4-methoxyphenyl)-5-phenyl-4,5-dihydro-1*H*-pyrazole (**7a**)

White powder; ^{1}H NMR (400.1 MHz, $CDCl_3$): δ_H 2.43 (CH_3), 3.17 (1H, dd, $^2J_{HH} = 17.8$, $^3J_{HH} = 4.8$ Hz, CH_2), 3.75 (1H, dd, $^2J_{HH} = 17.6$, $^3J_{HH} = 12.0$ Hz, CH_2), 3.79 (OCH_3), 5.57 (1H, dd, $^3J_{HH} = 12.0$, $^3J_{HH} = 4.8$ Hz, CH_2), 6.86 (2H, d, $^3J_{HH} = 8.0$ Hz, CH_{Ar}), 7.19 (2H, d, $^3J_{HH} = 8.0$ Hz, CH_{Ar}), 7.42–7.47 (3H, m, CH_{Ar}), 7.76–7.78 (2H, m, CH_{Ar}); ^{13}C NMR (100.6 MHz, $CDCl_3$): δ_C 22.0, 42.3, 55.3, 59.4, 114.2, 126.6, 126.9, 128.7, 130.3, 131.4, 134.1, 153.9, 159.0, 168.9.

2.5.11 | 1-Acetyl-5-(4-bromophenyl)-3-(4-methoxyphenyl)-4,5-dihydro-1*H*-pyrazole (**7b**)

Light yellow powder; ^{1}H NMR (400.1 MHz, $CDCl_3$): δ_H 2.42 (CH_3), 3.10 (1H, dd, $^2J_{HH} = 17.6$, $^3J_{HH} = 4.8$ Hz, CH_2), 3.73 (1H, dd, $^2J_{HH} = 17.6$, $^3J_{HH} = 12.0$ Hz, CH_2), 3.86 (OCH_3), 5.53 (1H, dd, $^3J_{HH} = 12.0$, $^3J_{HH} = 4.8$ Hz, CH_2), 6.95 (2H, d, $^3J_{HH} = 8.8$ Hz, CH_{Ar}), 7.13 (2H, d, $^3J_{HH} = 8.4$ Hz, CH_{Ar}), 7.44 (2H, d, $^3J_{HH} = 8.0$ Hz, CH_{Ar}), 7.69 (2H, d, $^3J_{HH} = 8.0$ Hz, CH_{Ar}); ^{13}C NMR (100.6 MHz, $CDCl_3$): δ_C 21.9, 42.2, 55.4, 59.3, 114.2, 121.4, 123.7, 127.4, 128.2, 131.9, 141.0, 153.6, 161.4, 168.7.

2.5.12 | 1-Acetyl-3,5-diphenyl-4,5-dihydro-1*H*-pyrazole (**7f**)

White powder; ^{1}H NMR (400.1 MHz, $CDCl_3$): δ_H 2.45 (CH_3), 3.19 (1H, dd, $^2J_{HH} = 17.8$, $^3J_{HH} = 4.4$ Hz, CH_2), 3.78 (1H, dd, $^2J_{HH} = 17.8$, $^3J_{HH} = 12.0$ Hz, CH_2), 5.62 (1H, dd, $^3J_{HH} = 12.0$, $^3J_{HH} = 4.4$ Hz, CH_2), 7.24–7.29 (3H, m, CH_{Ar}), 7.32–7.36 (2H, m, CH_{Ar}), 7.43–7.46 (3H, m, CH_{Ar}), 7.75–7.78 (2H, m, CH_{Ar}); ^{13}C NMR (100.6 MHz, $CDCl_3$): δ_C 21.9, 42.4, 59.9, 125.5, 126.6, 127.6, 128.7, 128.9, 130.3, 131.4, 141.8, 153.8, 168.9.

2.5.13 | 1-Acetyl-5-(4-methoxyphenyl)-3-phenyl-4,5-dihydro-1*H*-pyrazole (**7g**)

White powder; ^{1}H NMR (400.1 MHz, $CDCl_3$): δ_H 2.43 (CH_3), 3.17 (1H, dd, $^2J_{HH} = 17.8$, $^3J_{HH} = 4.4$ Hz, CH_2), 3.75 (1H, dd, $^2J_{HH} = 17.8$, $^3J_{HH} = 12.0$ Hz, CH_2), 3.79 (OCH_3), 5.57 (1H, dd, $^3J_{HH} = 12.0$, $^3J_{HH} = 4.4$ Hz, CH_2), 6.86 (2H, d, $^3J_{HH} = 8.4$ Hz, CH_{Ar}), 7.19 (2H, d, $^3J_{HH} = 8.4$ Hz, CH_{Ar}), 7.44–7.47 (3H, m, CH_{Ar}), 7.76–7.78 (2H, m, CH_{Ar}); ^{13}C NMR (100.6 MHz, $CDCl_3$): δ_C 22.0, 42.3, 55.3, 59.4, 114.2, 126.6, 126.9, 128.7, 130.3, 131.5, 134.1, 153.8, 159.0, 168.8.

2.5.14 | 1-Acetyl-5-(4-bromophenyl)-3-phenyl-4,5-dihydro-1*H*-pyrazole (**7j**)

Cream powder; ^{1}H NMR (400.1 MHz, $CDCl_3$): δ_H 2.45 (CH_3), 3.13 (1H, dd, $^{2}J_{HH} = 17.6$, $^{3}J_{HH} = 5.2$ Hz, CH_2), 3.76 (1H, dd, $^{2}J_{HH} = 17.6$, $^{3}J_{HH} = 12.0$ Hz, CH_2), 5.57 (1H, dd, $^{3}J_{HH} = 12.0$, $^{3}J_{HH} = 5.2$ Hz, CH_2), 7.12 (2H, d, $^{3}J_{HH} = 8.4$ Hz, CH_{Ar}), 7.44 (2H, d, $^{3}J_{HH} = 8.4$ Hz, CH_{Ar}), 7.45–7.46 (3H, m, CH_{Ar}), 7.74–7.76 (2H, m, CH_{Ar}); ^{13}C NMR (100.6 MHz, $CDCl_3$): δ_C 21.9, 42.2, 59.4, 125.6, 126.6, 127.4, 128.8, 128.9, 130.5, 132.0, 140.8, 153.9, 169.1.

2.5.15 | 1-Acetyl-5-(4-chlorophenyl)-3-phenyl-4,5-dihydro-1*H*-pyrazole (**7k**)

Cream powder; ^{1}H NMR (400.1 MHz, $CDCl_3$): δ_H 2.44 (CH_3), 3.14 (1H, dd, $^{2}J_{HH} = 17.8$, $^{3}J_{HH} = 4.4$ Hz, CH_2), 3.76 (1H, dd, $^{2}J_{HH} = 17.8$, $^{3}J_{HH} = 12.0$ Hz, CH_2), 5.57 (1H, dd, $^{3}J_{HH} = 12.0$, $^{3}J_{HH} = 4.4$ Hz, CH_2), 7.19 (2H, d, $^{3}J_{HH} = 8.4$ Hz, CH_{Ar}), 7.31 (2H, d, $^{3}J_{HH} = 8.4$ Hz, CH_{Ar}), 7.44–7.46 (3H, m, CH_{Ar}), 7.75–7.78 (2H, m, CH_{Ar}); ^{13}C NMR (100.6 MHz, $CDCl_3$): δ_C 21.9, 42.2, 59.3, 125.6, 127.1, 128.8, 129.0, 130.4, 131.2, 133.4, 140.3, 153.7, 168.9.

2.5.16 | 4-(1-Acetyl-3-phenyl-4,5-dihydro-1*H*-pyrazol-5-yl)benzonitrile (**7l**)

White powder; ^{1}H NMR (400.1 MHz, $CDCl_3$): δ_H 2.45 (CH_3), 3.14 (1H, dd, $^{2}J_{HH} = 17.8$, $^{3}J_{HH} = 5.2$ Hz, CH_2), 3.83 (1H, dd, $^{2}J_{HH} = 17.8$, $^{3}J_{HH} = 12.0$ Hz, CH_2), 6.63 (1H, dd, $^{3}J_{HH} = 12.0$, $^{3}J_{HH} = 5.2$ Hz, CH_2), 7.36 (2H, d, $^{3}J_{HH} = 8.4$ Hz, CH_{Ar}), 7.45–7.48 (3H, m, CH_{Ar}), 7.64 (2H, d, $^{3}J_{HH} = 8.4$ Hz, CH_{Ar}), 7.74–7.77 (2H, m, CH_{Ar}); ^{13}C NMR (100.6 MHz, $CDCl_3$): δ_C 21.9, 42.0, 59.6, 111.6, 118.5, 126.5, 126.6, 128.8, 130.7, 132.8, 146.8, 153.8, 169.1.

2.5.17 | 1-Acetyl-5-(4-nitrophenyl)-3-phenyl-4,5-dihydro-1*H*-pyrazole (**7m**)

Yellow powder; ^{1}H NMR (400.1 MHz, $CDCl_3$): δ_H 2.46 (CH_3), 3.16 (1H, dd, $^{2}J_{HH} = 17.8$, $^{3}J_{HH} = 4.0$ Hz, CH_2), 3.86 (1H, dd, $^{2}J_{HH} = 17.8$, $^{3}J_{HH} = 12.0$ Hz, CH_2), 5.68 (1H, dd, $^{3}J_{HH} = 12.0$, $^{3}J_{HH} = 4.0$ Hz, CH_2), 7.43 (2H, d, $^{3}J_{HH} = 8.4$ Hz, CH_{Ar}), 7.44–7.49 (3H, m, CH_{Ar}), 7.75–7.77 (2H, m, CH_{Ar}), 7.75–7.77 (2H, m, CH_{Ar}), 8.21 (2H, d, $^{3}J_{HH} = 8.4$ Hz, CH_{Ar}); ^{13}C NMR (100.6 MHz, $CDCl_3$): δ_C 21.8, 42.1, 59.4, 124.3, 126.6, 126.7, 128.8, 130.7, 130.8, 147.4, 148.8, 153.7, 169.1.

2.5.18 | 1-Acetyl-5-(4-nitrophenyl)-3-phenyl-4,5-dihydro-1*H*-pyrazole (**7n**)

Orange powder; ^{1}H NMR (400.1 MHz, $CDCl_3$): δ_H 2.46 (CH_3), 3.17 (1H, dd, $^{2}J_{HH} = 17.6$, $^{3}J_{HH} = 5.6$ Hz, CH_2), 3.86 (1H, dd, $^{2}J_{HH} = 17.6$, $^{3}J_{HH} = 12.0$ Hz, CH_2), 5.68 (1H, dd, $^{3}J_{HH} = 12.0$, $^{3}J_{HH} = 5.6$ Hz, CH_2), 7.43 (2H, d, $^{3}J_{HH} = 8.8$ Hz, CH_{Ar}), 7.43–7.46 (1H, m, CH_{Ar}), 7.46–7.47 (2H, m, CH_{Ar}), 7.75–7.77 (2H, m, CH_{Ar}), 7.75–7.77 (2H, m, CH_{Ar}), 8.21 (2H, d, $^{3}J_{HH} = 8.8$ Hz, CH_{Ar}); ^{13}C NMR (100.6 MHz, $CDCl_3$): δ_C 21.8, 42.0, 59.4, 124.2, 124.3, 126.6, 126.7, 128.6, 128.8, 128.9, 130.7, 148.8, 169.1.

2.5.19 | 4-(1-Acetyl-5-phenyl-4,5-dihydro-1*H*-pyrazol-3-yl)benzonitrile (**7o**)

White powder; ^{1}H NMR (400.1 MHz, $CDCl_3$): δ_H 2.45 (CH_3), 3.15 (1H, dd, $^{2}J_{HH} = 17.6$, $^{3}J_{HH} = 4.8$ Hz, CH_2), 3.82 (1H, dd, $^{2}J_{HH} = 17.6$, $^{3}J_{HH} = 12.0$ Hz, CH_2), 5.62 (1H, dd, $^{3}J_{HH} = 12.0$, $^{3}J_{HH} = 4.8$ Hz, CH_2), 7.37 (2H, d, $^{3}J_{HH} = 8.4$ Hz, CH_{Ar}), 7.45–7.48 (3H, m, CH_{Ar}), 7.64 (2H, d, $^{3}J_{HH} = 8.4$ Hz, CH_{Ar}), 7.74–7.77 (2H, m, CH_{Ar}); ^{13}C NMR (100.6 MHz, $CDCl_3$): δ_C 21.9, 42.1, 59.6, 111.6, 118.6, 126.5, 126.6, 128.8, 130.7, 130.8, 132.8, 146.9, 153.7, 169.0.

3 | RESULTS AND DISCUSSION

Amine-functionalized nanozeolite (ZeSi–AP) was synthesized by reacting nanozeolite with CPTMS to generate silane-functionalized nanozeolite (ZeSi), which then treated with AP to afford the expected solid catalyst ZeSi–AP as depicted in Scheme 2. The structure of the catalyst

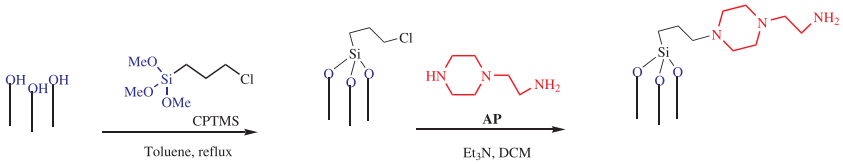

SCHEME 2 Synthesis of the catalyst ZeSi–AP

was characterized by FT-IR, TGA, DTA, XRD, SEM, and TEM techniques.

Figure 1 shows the FT-IR spectra of Ze, ZeSi, AP, and ZeSi–AP. The spectra of Ze, ZeSi, and ZeSi–AP exhibit characteristic bands at 3300–3600, 1640, and 1095 cm^{-1} corresponding to O—H stretching, O—H bending, and Si—O stretching vibrations, respectively. Additional absorption peaks at about 2957 cm^{-1} related to the C—H stretching vibrations of the methylene groups of propyl chloride in the spectrum of ZeSi confirm the successful attachment of the CPTMS group into the Ze surface. The IR spectrum of AP shows the expected bands at 3486 cm^{-1} related to N—H stretching vibrations of the amine groups, 2800–2925 cm^{-1} associated with the C—H stretching, 1647 and 1458 cm^{-1} that are corresponding to NH_2 bending of the amine groups.[5a,b]

The IR spectrum of ZeSi–AP displays absorption bands at 3565 cm^{-1} (N—H stretching vibration), 1640 and 1458 cm^{-1} (NH_2 bending vibrations), and 1100 cm^{-1} (Si—O—Si stretching vibration) confirming the successful synthesis of aminoethyl piperazine functionalized nanozeolite.

Thermogravimetric analysis (TGA) of the Ze, ZeSi, and ZeSi–AP is depicted in Figure 2. The heating range from 30°C to 600°C with a rate of 10°C/min was applied for all samples. As it can be seen in Figure 2 and DTA of the samples (Figure 3), the thermogram of Ze displays a weight loss at >200°C, which is related to physically absorbed surface water. The TGA profile of ZeSi shows a weight loss at >150°C that is attributed to the physisorbed surface water and a weight loss at 275–300°C, which is related to the removal of the organic chloropropyl groups. The TGA curve of ZeSi–AP represents two weight losses at <110°C and at 200–400°C, which can be due to the removal of surface water and of organic aliphatic amine groups, respectively.

According to the TGA data, the amount of loaded amine onto the nanozeolite surface was calculated to be around 1.43 mmol/g. Further, the results of CHN analysis of ZeSi and ZeSi–AP shown in Table 1 reveal that the higher percent of carbon atom and presence of nitrogen atom in the structure of ZeSi–AP comparing with ZeSi could certainly approve the successful immobilization of AP on the nanozeolite. The amount of loaded AP was calculated to be nearly 1.39 mmol/g from data in Table 1, which is in good agreement with that obtained from TGA.

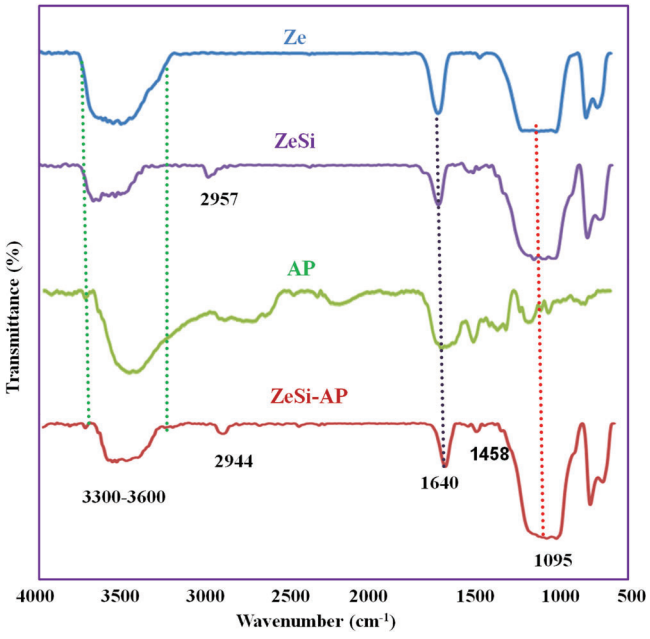

FIGURE 1 IR spectra of the Ze, ZeSi, AP, and ZeSi–AP

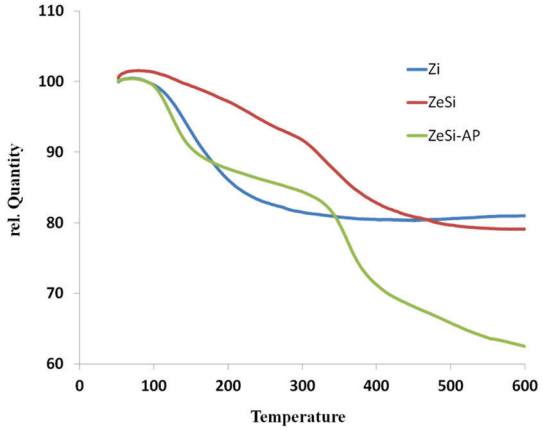

FIGURE 2 The TGA thermograms of Ze, ZeSi, and ZeSi–AP

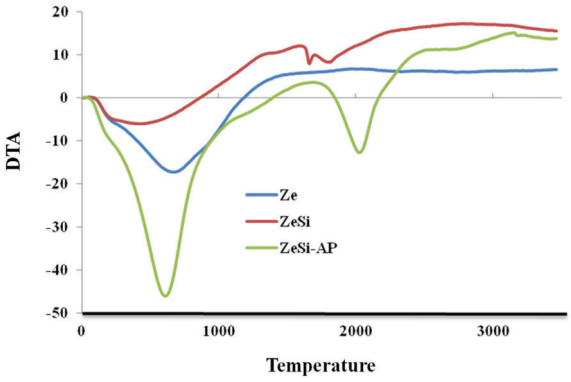

FIGURE 3 The DTA thermograms of Ze, ZeSi, and ZeSi–AP

TABLE 1 The results of ZeSi and ZeSi–AP CHN analysis

Entry	Catalyst	C (wt %)	N (wt %)
1	ZeSi	7.21	—
2	ZeSi–AP	17.2	5.83

The morphology of the catalyst was characterized by SEM and TEM images as demonstrated in Figures 4 and 5, respectively. As it can be seen in these figures, the similarity of SEM and TEM images of Ze, ZeSi, and ZeSi–AP indicates that the surface of NaY nanozeolite has not been significantly changed during the immobilization process. The mean particle sizes were calculated to be ~20–90 nm as specified in Figures 4 and 5.

Moreover, elemental mapping of the ZeSi–AP approves the presence of Al, Si, O, C, N, and O atoms in the nanozeolite structure (Figure 6) and confirms that

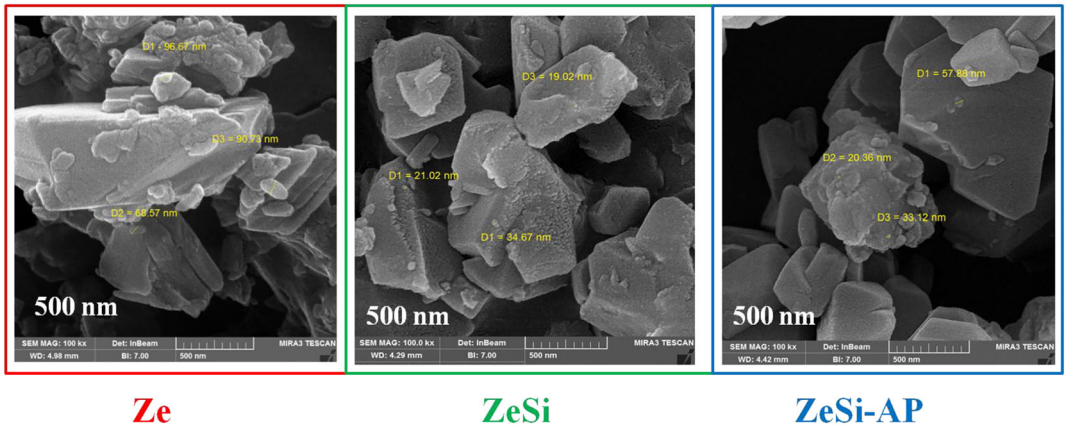

FIGURE 4 SEM images of Ze, ZeSi, and ZeSi–AP

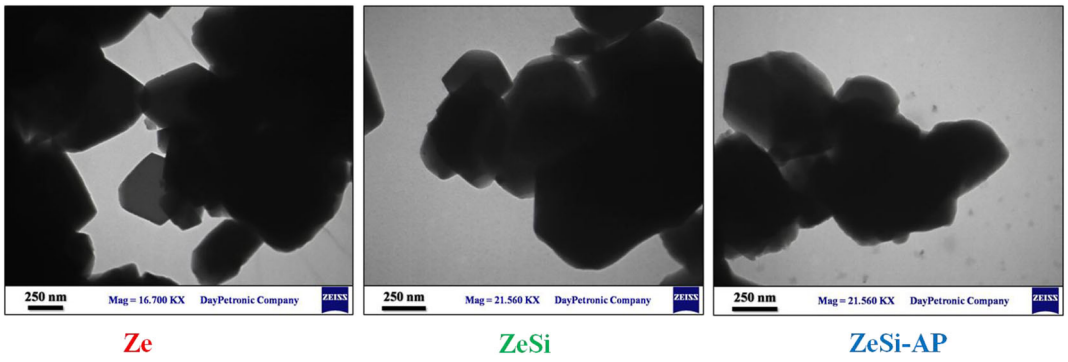

FIGURE 5 TEM images of Ze, ZeSi, and ZeSi–AP

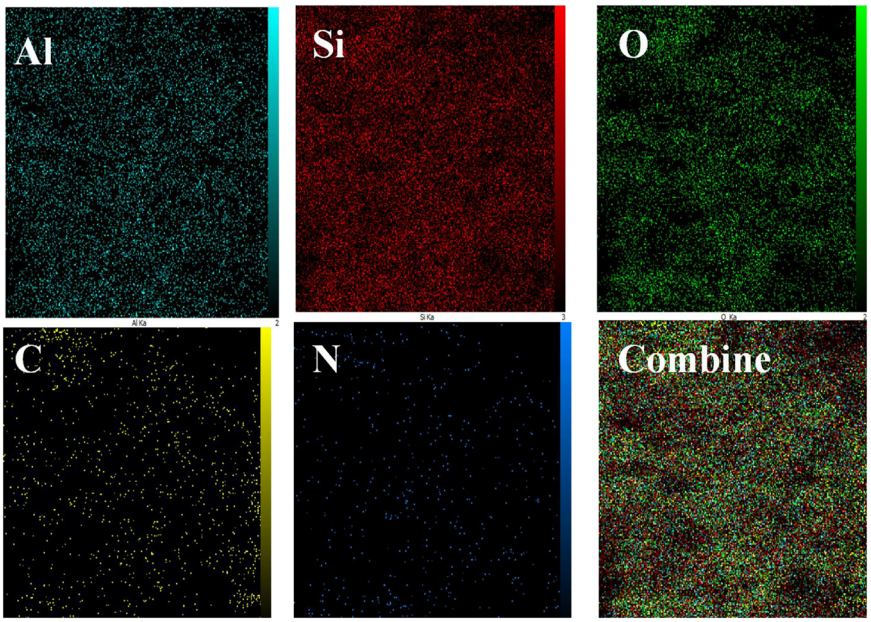

FIGURE 6 Elemental mapping of the ZeSi–AP, revealing the elemental distributions of Al, Si, O, C, and N

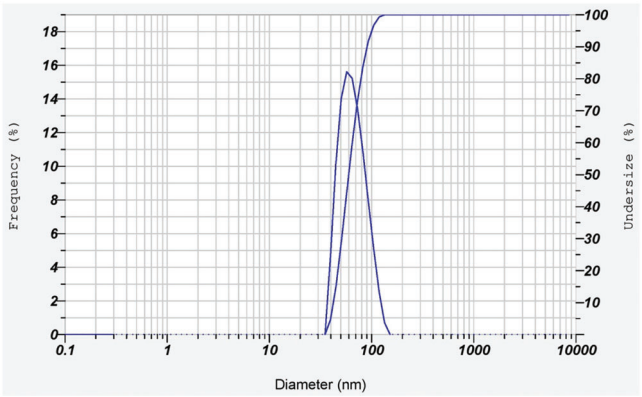

FIGURE 7 The DLS results of the ZeSi–AP

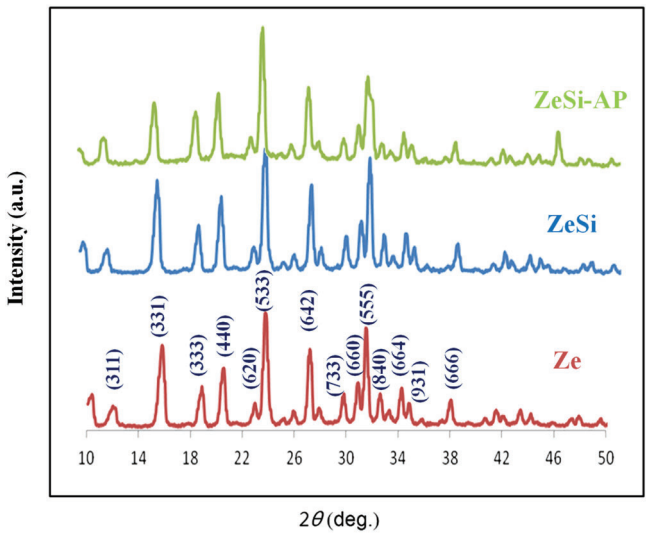

FIGURE 8 XRD patterns of Ze, ZeSi, and ZeSi–AP

the elements are uniformly distributed in the catalyst surface.

Besides, the DLS analysis was performed to determine the hydrodynamic diameter and particle size distribution of ZeSi–AP (Figure 7). According to the DLS data, the average particle size of the ZeSi–AP was found to be 64 nm with a narrow particle size distribution. The results of DLS analysis are in good agreement with the results of XRD and SEM analyses.

The crystal structure of Ze, ZeSi, and ZeSi–Ap were studied by X-ray diffraction using a Cu Kα irradiation as depicted in Figure 8. The diffraction pattern of the annealed samples matched well with NaY zeolite structure (Reference Code 98-010-5558 $Na_2Al_2Si_5O_{13}{\cdot}xH_2O$). In the range of the 2θ (10–50), nano-NaY zeolite exhibited all the characteristic reflections: (311), (331), (333), (440), (620), (533), (642), (733), (660), (555), (840), (664), (931), and (666). The similarity of the XRD diffraction patterns of Ze, ZeSi, and ZeSi–AP certainly demonstrates that the crystal structure of NaY nanozeolite (Ze) has not been destroyed during functionalization with CPTMS and AP, which is in good agreement with the results of TEM and SEM analyses.[15]

Figure 9 exhibits the N_2 adsorption–desorption isotherms of all samples, and data extracted from BET and t-plot including total specific surface area (S_{BET}), total specific surface area (a_1), external specific surface area (a_2), and micropore area (a_1–a_2) are tabulated in Table 2. The isotherms of Ze, ZeSi, and ZeSi–AP were type I, which is characteristic of the microporous structures.[15b,c] It is clear from Table 2 that the specific surface area, total specific surface area (a_1), external

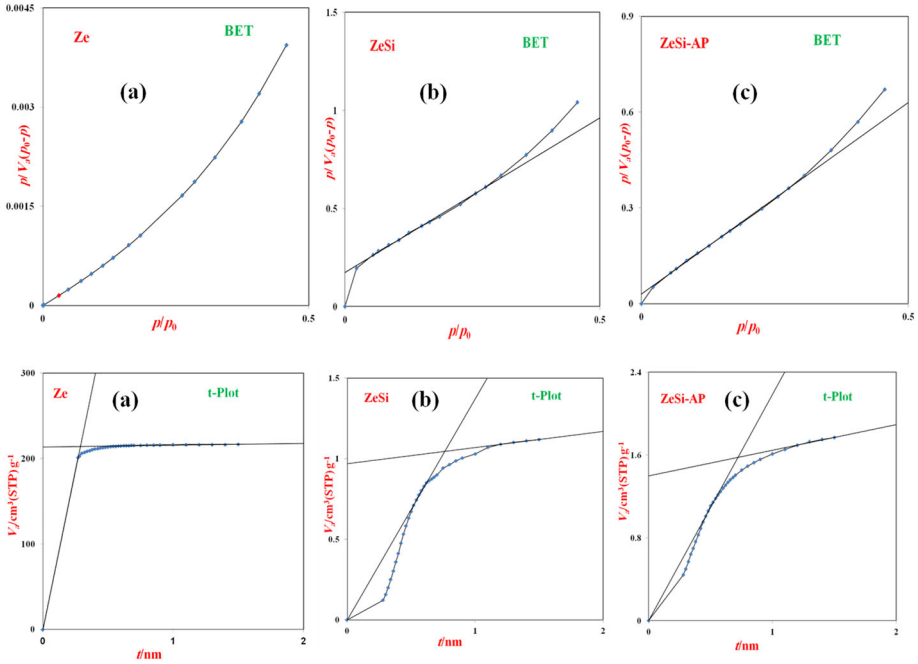

FIGURE 9 BET and t-plot of Ze (a), ZeSi (b), and ZeSi–AP (c)

specific surface area (a_2), and micropore area (a_1–a_2) are reduced from Ze to ZeSi and ZeSi–AP. These drastic reductions in the surface area and pore volumes for ZeSi and ZeSi–AP compared with Ze could be due to attachment of organic molecules to the surface of the zeolite, which could cause blockage and narrowing of the zeolite pores and openings.[15d,e] Also, the amine density on the surface of the ZeSi–AP was calculated to be 2.36 amines/Å^2 based on the CHN and BET analyses.

The catalytic activity of the amine functionalized NaY zeolite (ZeSi–AP) was studied in the reaction of aromatic aldehyde **1**, ethyl acetoacetate **2**, and either urea or thiourea **3** in the presence of catalytic amount of the ZeSi–AP to obtain DHPM derivative **4** (Scheme 3).

The reaction of benzaldehyde **1a** (2 mmol), ethyl acetoacetate **2** (2 mmol), and urea **3a** (2.5 mmol) in the presence of nanocatalyst in 10-ml ethanol was chosen as a model reaction to achieve the optimal reaction conditions. As it is clear in Table 3, the model reaction in the

TABLE 2 Data obtained from N_2 adsorption–desorption isotherms

Catalyst	BET Total specific surface area (S_{BET}, m^2/g)	t-plot Total specific surface area (a_1, m^2/g)	t-plot External specific surface area (a_2, m^2/g)	t-plot Micropore area (a_1–a_2, m^2/g)
Ze	872.36	1147.0	3.07	1143.93
ZeSi	248.9	211.3	1.54	209.76
ZeSi–AP	3.54	3.36	0.38	2.98

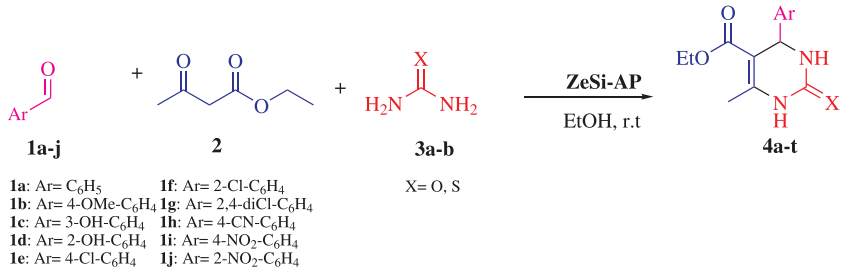

SCHEME 3 Synthesis of DHPM derivatives using ZeSi–AP

TABLE 3 Optimization of reaction conditions for the synthesis of DHPMs

Entry	Catalyst (mg)	Solvent	Temperature (°C)	Time (min)	Yield %[a,b]
1	Ze (10)	EtOH	80	120	trace
2	ZeSi (10)	EtOH	80	120	trace
3	ZeSi–AP (10)	EtOH	r.t	40	72
4	ZeSi–AP (10)	EtOH	40	40	74
5	ZeSi–AP (10)	EtOH	80	40	74
6	ZeSi–AP (15)	EtOH	r.t	40	79
7	ZeSi–AP (20)	EtOH	r.t	40	92
8	ZeSi–AP (25)	EtOH	r.t	40	92
9	ZeSi–AP (30)	EtOH	r.t	40	92
10	ZeSi–AP (20)	EtOH:H_2O	r.t	90	65
11	ZeSi–AP (20)	H_2O	r.t	120	47
12	ZeSi–AP (20)	MeOH	r.t	60	68
13	ZeSi–AP (20)	THF	r.t	60	63
14	ZeSi–AP (20)	Et_2O	r.t	60	45

[a]Reaction conditions: benzaldehyde (2 mmol), ethyl acetoacetate (2 mmol), and urea (2.5 mmol) in the presence of catalyst in 10-ml solvent.
[b]Isolated yields.

presence of Ze and ZeSi afforded only a trace amount of the DHPM **4a** in refluxing ethanol after 2 h, whereas in the presence of ZeSi–AP, the reaction yield increased to 72% in ethanol at room temperature after 40 min indicating the role of the ZeSi–AP in this reaction (Entries 1–3). Increasing temperature did not improve the product yield

TABLE 4 Comparison of the catalyst ZeSi–AP with those reported in the literature

Entry	Catalyst/amount	Conditions	Time (min)	Yield (%)
1	β-Cyclodextrine/0.5 mol%	Solvent-free/100°C	180	85[16a]
2	Cellulose sulfuric acid/0.05 g	CH_3CN/100°C	270	80[16b]
3	12-Molybdophosphoric acid/2 mol%	AcOH/reflux	300	80[16c]
4	Silica sulfuric acid/0.23 g	EtOH/reflux	360	91[16d]
5	Silica gel-supported L-pyrrolidine-2-carboxylic acid-4-hydrogen sulfate/212 mg	EtOH/reflux	360	92[16e]
6	Amberlyst-70/50 mg	H_2O/90°C	180	81[16f]
7	Poly(4-vinylpyridine-co-divinylbenzene)–Cu(II)/20 wt%	MeOH/reflux	24 h	70[16g]
8	12-Tungstophosphoric acid/2 mol%	AcOH/reflux	360	75[16h]
9	Fe_3O_4@camphor/0.02 g	EtOH/r.t	85	77[16i]
10	$CoFe_2O_4$/TMU-17-NH_2/20 mg	Solvent-free/80°C	30	98[16j]
11	ZeSi–AP/20 mg	EtOH/r.t	40	92[a]

[a]This work.

TABLE 5 Synthesis of DHPM derivatives

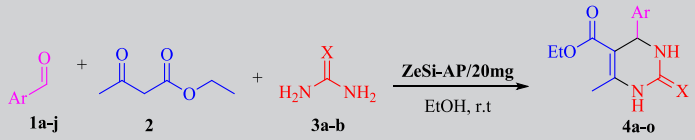

Product	Ar	X	Time (min)	Yield (%)[a]	TON[b]/TOF (h)[c]	Mp (°C)
4a	C_6H_5	O	40	92	66/100	207–210[16d]
4b	4-OMe—C_6H_4	O	30	92	66/132	200–202[16d]
4c	3-OH—C_6H_4	O	30	88	63/126	162–165[16d]
4d	2-OH—C_6H_4	O	45	85	61/81	198–201[16g]
4e	4-Cl—C_6H_4	O	60	90	65/65	213–215[16d]
4f	2-Cl—C_6H_4	O	10	87	62/391	213–216[16g]
4g	2,4-diCl—C_6H_3	O	60	95	68/68	250–251[16d]
4h	4-CN—C_6H_4	O	30	94	68/135	176–179[16a]
4i	4-NO_2—C_6H_4	O	30	90	65/129	207–208[16d]
4j	2-NO_2—C_6H_4	O	30	85	61/122	223–225[16d]
4k	C_6H_5	S	40	86	62/94	207–209[16d]
4l	2-NO_2—C_6H_4	S	40	82	59/89	220–222[16e]
4m	3-OH—C_6H_4	S	60	80	56/56	180–182[16d]
4n	4-Cl—C_6H_4	S	40	83	60/91	181–183[16e]
4o	4-CN—C_6H_4	S	60	86	62/62	236–238[16a]

[a]Isolated yields.
[b]TON = moles of product formed/moles of loaded amine in the catalyst (based on CHN).
[c]TOF = TON per time (h).

(Entries 4 and 5). Increasing the catalyst loading to 15, 20, 25, and 30 mg gave a reaction yield of 92%, and 20 mg of catalyst loading was chosen as optimal value (Entries 6–9). After optimization of catalyst loading, the model reaction was screened in different solvents like EtOH:H_2O, H_2O, EtOH, MeOH, THF, and Et_2O (Entries 7 and 10–14), and the results in Table 3 indicate that ethanol is the best solvent for this reaction (Entry 7).

In order to demonstrate the merit of the present catalytic method for the preparation of DHPMs, the model reaction was compared with some of the catalysts previously reported in the literature (Table 4). It is clear from this table that the model reaction with β-cyclodextrin and $CoFe_2O_4$/TMU-17-NH2 as catalysts afforded **4a** in 85% and 98% yields under solvent-free conditions at 100°C and 80°C after 3 h and 30 min, respectively (Entries 1 and 10). The other catalysts such as cellulose sulfuric acid (Entry 2), 12-molybdophosphoric acid (Entry 3), silica sulfuric acid (Entry 4), silica gel-supported L-pyrrolidine-2-carboxylic acid-4-hydrogen sulfate (Entry 5), amberlyst-70 (Entry 6), poly(4-vinylpyridine-co-divinylbenzene)–Cu(II) complex (Entry 7), and 12-tungstophosphoric acid (Entry 8) afforded the product (**4a**) in 70–92% yields at reflux temperature of the related solvents after 3–24 h. Fe_3O_4@camphor gave **4a** in 77% yield at room temperature after 85 min (Entry 9). However, the introduced catalyst performed the model reaction at room temperature and product (**4a**) was obtained in 92% yield after 40 min (Entry 11).

To demonstrate the merit of this method, various aldehydes **1** were treated with ethyl acetoacetate **2** and urea or thiourea **3** under optimal conditions, and the results were tabulated in Table 5. Both electron-donating and electron-withdrawing substituents in the aromatic ring of the benzaldehyde afforded reasonable yields of the related products (Entries 1–14). All the synthesized compounds have been already reported in the literature, and their structures were confirmed by comparing their physical and ^1H and ^{13}C NMR spectral data with those reported in the literature.

A plausible mechanism is presented in Scheme 4 for the formation of DHPMs **4**. It appears that the initial event involves the nucleophilic attack of urea **3a** to aldehyde **1** to generate the intermediate **8**, which then eliminates one molecule of water to produce intermediate **9**. Then the Michael-type addition of enol **2** to intermediate **9** gives **10**, which subsequently undergoes heterocyclization to provide the relevant product **4**.[16]

The results of the above reaction to prepare DHPMs encouraged us to investigate the catalytic activity of the synthesized ZeSi–AP in the preparation of *N*-acetyl pyrazole derivatives (Scheme 5). Treatment of chalcone **5f** (2 mmol) with acyl hydrazine **6** (2.4 mmol) was selected as a reference reaction and screened under different reaction conditions to achieve the highest yield of the products **7a–n**, and results are displayed in Table 6. The model reaction in the presence of either Ze or ZeSi (10 mg) at 80°C generated only trace amount of the product after 2 h, whereas in the presence of ZeSi–AP (10 mg) gave 42% yield at room temperature after 1 h (Entries 1–3). Increasing temperature to 40°C, 50°C, and 60°C increased the reaction yield to 64% after 1 h (Entries 4–6), though higher temperature did not improve the yield (Entry 7). The catalyst loading from 10 to 15, 20, 25, and 30 mg was investigated (Entries 8–11), and the optimum amount of catalyst was determined to be 25 mg to achieve the highest product yield (Entry 10). The model

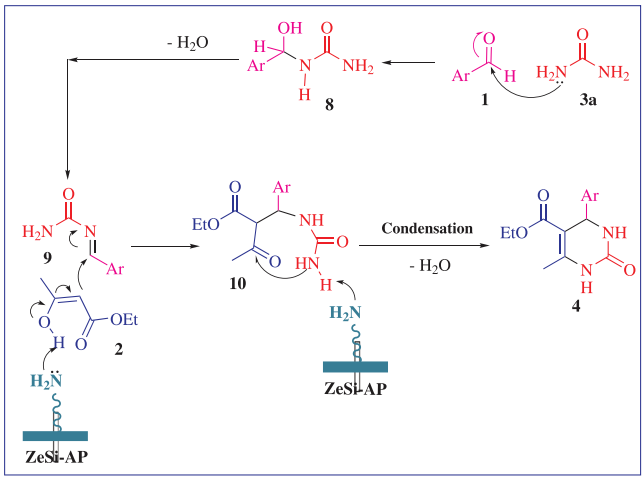

SCHEME 4 The plausible mechanism for the preparation of DHPMs

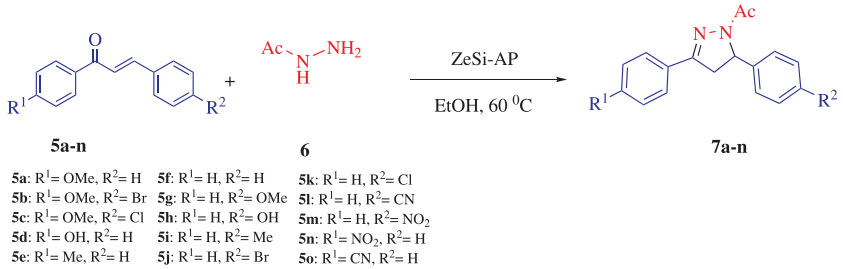

SCHEME 5 Synthesis of *N*-acetyl pyrazole derivatives using ZS–AP

TABLE 6 Optimization of reaction conditions for the synthesis of *N*-acetyl pyrazoles

Entry	Catalyst (mg)	Solvent	Temperature (°C)	Time (min)	Yield %[a,b]
1	Ze (10)	EtOH	80	120	trace
2	ZeSi (10)	EtOH	80	120	trace
3	ZeSi–AP (10)	EtOH	r.t	60	42
4	ZeSi–AP (10)	EtOH	40	60	47
5	ZeSi–AP (10)	EtOH	50	60	55
6	ZeSi–AP (10)	EtOH	60	60	64
7	ZeSi–AP (10)	EtOH	80	60	64
8	ZeSi–AP (15)	EtOH	60	60	73
9	ZeSi–AP (20)	EtOH	60	60	81
10	ZeSi–AP (25)	EtOH	60	60	94
11	ZeSi–AP (30)	EtOH	60	60	94
12	ZeSi–AP (25)	EtOH:H_2O	60	60	67
13	ZeSi–AP (25)	H_2O	60	60	45
14	ZeSi–AP (25)	THF	60	60	52

[a]Reaction conditions: chalcone (2 mmol), acylhydrazine (2.4 mmol), catalyst, and solvent (5 ml).
[b]Isolated yields.

TABLE 7 Comparison of the ZeSi–AP with other catalytic systems in the preparation of **7e**

Entry	Catalyst/amount	Conditions	Time (h)	Yield (%)
1	Fly ash H_2SO_4/0.4 g	MW/solvent-free	0.1	77[11b]
2	PS-DIEA/1 g	EtOH/r.t	12	78[14]
3	$Sc(OTf)_3$/5 mol%	MW/solvent-free/100°C	4	74[13]
4	Methanesulfonic acid/1 equiv	EtOH/reflux	0.75	95[13]
5	SiO_2Cl/30 mol%	Solvent-free/120°C	2	80[13]
6	TBD/0.1 equiv	CH_3CN/60°C	24 h	89[13]
7	KOH/1 equiv	EtOH/reflux	5	90[13]
8	$Pd(OAc)_2$–K_2CO_3/5 mol%	1,4-Dioxane:water/100°C	8 h	60[13]
9	ZeSi–AP	EtOH/60°C	1	94[a]

[a]This work.

reaction in the presence of ZeSi–AP (25 mg) in different solvents such as EtOH:H_2O (1:1), H_2O, and THF under the same reaction conditions (60°C, 1 h) led to lower yield of the product **7e** (Entries 12–14).

The advantages of ZeSi–AP in comparison with the reported catalytic systems for the preparation of *N*-acetyl pyrazoles were displayed in Table 7. As can be seen, the amine-modified NaY nanozeolite promoted the model reaction smoothly based on reaction time and yield. According to Table 7 fly ash H_2SO_4 was employed as an acidic catalyst under solvent-free conditions. This system affords the *N*-acetyl pyrazoles in short time but in low yield (Entry 1). In the case of polymer bound (*N*,*N*-(diisopropyl)aminomethyl polystyrene [PS-DIEA]), a long reaction time is required to obtain only low product yield (Entry 2). Using other catalysts, such as $Sc(OTf)_3$ (Entry 3), methanesulfonic acid (Entry 4), SiO_2Cl (Entry 5), 1,5,7-triazabicyclo[4.4.0]dec-5-ene (TBD) (Entry 6), KOH (Entry 7), and palladium acetate (5 mol%) (together with SPhos [10 mol%] and K_2CO_3 [2 M]) (Entry 8), results low product yield in time-consuming reaction. It is clear that the introduced catalytic system could be substantially used under mild and green conditions to give high product yield in short reaction time (Entry 9).

To extend the reaction scope, different chalcones **5b–o** were treated with acyl hydrazine **6** to obtain *N*-acetyl pyrazoles **7b–o**. Table 8 shows that chalcones with different substituents tolerate in this reaction and

TABLE 8 Preparation of *N*-acyl pyrazoles

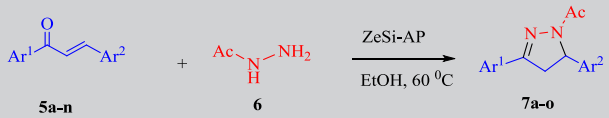

Product	Ar^1	Ar^2	Time (min)	Yield (%)[a]	TON[b]/TOF (h)[c]	Mp (°C)
7a	4-OMe—C_6H_4	C_6H_5	60	84	48/48	133–135[17a]
7b	4-OMe—C_6H_4	4-Br—C_6H_4	60	88	51/51	262–264
7c	4-OMe—C_6H_4	4-Cl—C_6H_4	60	85	49/49	172–174[17b]
7d	4-OH—C_6H_4	C_6H_5	75	81	47/38	212–214[17c]
7e	2-OMe—C_6H_4	C_6H_5	75	82	47/37	128–130[17a]
7f	C_6H_5	C_6H_5	60	94	54/54	119–121[11b]
7g	C_6H_5	4-OMe—C_6H_4	75	79	45/36	74–76[17d]
7h	C_6H_5	4-OH—C_6H_4	90	77	44/29	210–213[17e]
7i	C_6H_5	4-Me—C_6H_4	75	84	48/39	108–110[11b]
7j	C_6H_5	4-Br—C_6H_4	60	87	50/50	118–120[17f]
7k	C_6H_5	4-Cl—C_6H_4	60	85	49/49	107–109[11b]
7l	C_6H_5	4-CN—C_6H_4	50	93	53/64	115–117
7m	C_6H_5	4-NO_2—C_6H_4	50	94	54/65	163–165[11b]
7n	4-NO_2—C_6H_4	C_6H_5	60	86	50/50	192–194[17g]
7o	4-CN—C_6H_4	C_6H_5	60	83	48/48	200–201

[a]Isolated yields.
[b]TON = moles of product formed/moles of loaded amine in the catalyst (based on CHN).
[c]TOF = TON per time (h).

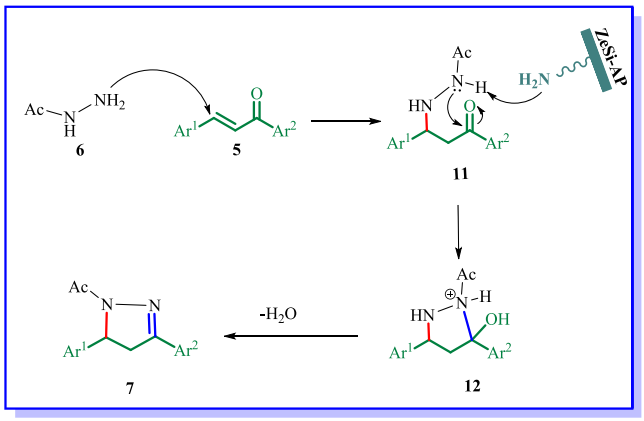

SCHEME 6 The suggested mechanism for preparation of *N*-acetyl pyrazoles catalyzed by ZeSi–AP

high yield of corresponding products is obtained (Entries 1–14). All the synthesized *N*-acyl pyrazoles are known and characterized with their melting point, ^{1}H NMR, and ^{13}C NMR spectra and comparison with data reported in the literature.

According to the literature review, a tentative mechanism is depicted in Scheme 6. It is assumed that the ZeSi–AP enhanced the nucleophilic attack of acyl hydrazine **6** to carbonyl carbon of chalcone **5** generating intermediate **11**, which then eliminates one molecule of water to give intermediate **12**. Intramolecular nucleophilic attack of nitrogen atom of acyl hydrazine to beta carbon of chalcone in **12** and subsequent dehydration leads to five-membered pyrazole ring **7**.[17a]

It is noteworthy to mention that in this catalytic method, the catalyst is easily recovered and reused for several runs. Figure 10 exhibits the recyclability of nano-ZeSi–AP up to four cycles in the model reaction, which certainly demonstrates the excellent catalytic performance of the synthesized catalyst. The SEM image of recycled ZeSi–AP after fourth consecutive cycles in Figure 11 is similar to fresh catalyst (Figure 4) indicating no significant change in the surface of the catalyst. To explore the catalyst leaching, the reaction between benzaldehyde, ethyl acetoacetate, and urea was carried out under optimized conditions. After 20 min (half of needed time for completion of reaction), the reaction was

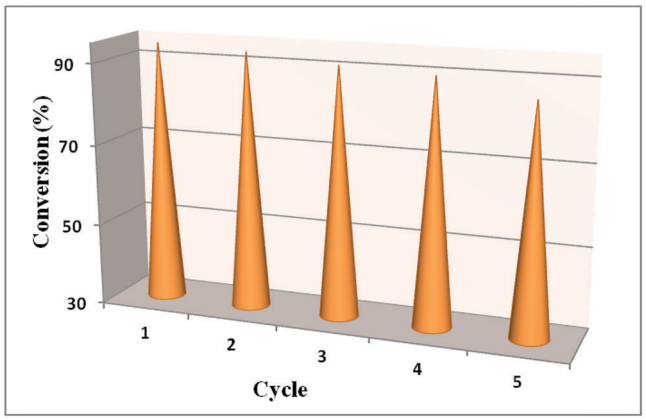

FIGURE 10 Catalyst reusability in the model reaction

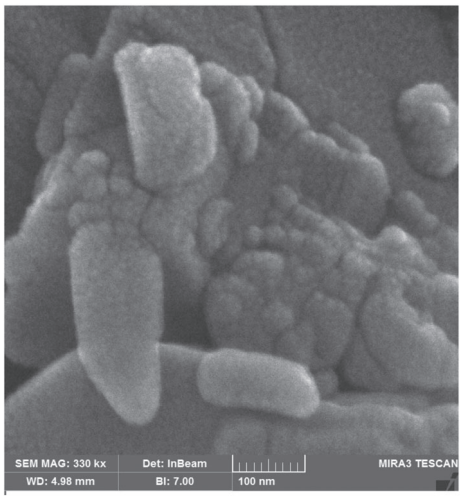

FIGURE 11 SEM images of reused ZeSi–AP (after four cycles)

stopped and the catalyst was separated. The yield of product was measured by GC (74%). The residue was then allowed to react without catalyst for another 60 min. After that, the reaction mixture was analyzed by GC, and the result showed that no significant conversion was observed after catalyst separation.

4 | CONCLUSIONS

In summary, 1-(2-aminoethyl)piperazine-modified nano-NaY zeolite was simply synthesized by reacting NaY nanozeolite with CPTMS followed by treating with 1-(2-aminoethyl)piperazine to afford ZeSi–AP. The structure of the catalyst was identified by using FT-IR, XRD, TGA, DTA, DLS, SEM, TEM, and elemental analyses. The catalytic activity of the synthesized catalyst was investigated in the synthesis of DHPMs and *N*-acetyl pyrazoles. The results indicated the efficacy of this catalyst in both reactions. It is suggested that this catalytic system can be utilized for preparation of other important heterocycles systems under mild and green conditions.

ACKNOWLEDGMENTS

The authors are thankful to the University of Mazandaran and Islamic Azad University, Tehran North Branch, for partial support of this project.

CONFLICT OF INTERESTS

The authors declare that there is no conflict of interest.

AUTHOR CONTRIBUTIONS

Raheleh Razavian Mofrad: Conceptualization; data curation; formal analysis; investigation; methodology; project administration; resources. **Hassan Kabirifard:** Conceptualization; funding acquisition; project administration; supervision. **Mahmood Tajbakhsh:** Conceptualization; data curation; formal analysis; funding acquisition; investigation; methodology; project administration; resources; supervision; validation. **Ghasem Firouzzadeh Pasha:** Conceptualization; data curation; formal analysis; funding acquisition; investigation; methodology; resources; software; supervision; validation; visualization.

ORCID

Raheleh Razavian Mofrad https://orcid.org/0000-0002-7536-5544

Hassan Kabirifard https://orcid.org/0000-0003-2680-8051

Mahmood Tajbakhsh https://orcid.org/0000-0002-4856-1937

Ghasem Firouzzadeh Pasha https://orcid.org/0000-0002-5054-2938

REFERENCES

[1] a) M. J. Climent, A. Corma, S. Iborra, *Chem. Rev.* **2011**, *111*, 1072; b) I. T. Horváth, T. A. Paul, *Chem. Rev.* **2007**, *107*, 2167; c) J. M. Lee, Y. Na, H. Han, S. Chang, *Chem. Soc. Rev.* **2004**, *33*, 302.

[2] a) J. C. Wasilke, S. J. Obrey, R. T. Baker, G. C. Bazan, *Chem. Rev.* **2005**, *105*, 1001; b) C. de Graaff, E. Ruijter, R. V. Orru, *Chem. Soc. Rev.* **2012**, *41*, 3969; c) B. B. Toure, D. G. Hall, *Chem. Rev.* **2009**, *109*, 4439.

[3] a) S. Montalvo, L. Guerrero, R. Borja, E. Sánchez, Z. Milán, I. Cortés, M. A. Rubia, *Appl. Clay Sci.* **2012**, *58*, 125; b) S. Rezvantalab, F. Bahadori, *Asian J. Agric. Res.* **2015**, *9*(6), 343; c) C. Li, M. Moliner, A. Corma, *Angew. Chem., Int. Ed.* **2018**, *57*, 15330; d) J. Přech, *Catal. Rev.: Sci. Eng.* **2018**, *60*, 71; e) A. A. Dabbawala, V. Tzitzios, K. Sunny, K. Polychronopoulou, G. Basina, I. Ismail, S. M. Alhassan, *Surf. Coat. Technol.* **2018**, *350*, 369.

[4] a) S. Męczyńska, A. Piotrowska, A. Majkowska, A. Bilewicz, M. Kruszewski, *Nanoscale Res. Lett.* **2016**, *11*, 1; b) F. Babaei, S. Asghari, M. Tajbakhsh, *Res. Chem. Intermed.* **2019**, *45*, 4693; c) D. H. Lee, M. Choi, B. W. Yu, R. Ryoo, *Chem. Commun.* **2009**, *1*, 74; d) A. Corma, H. Garcia, *Adv. Synth. Catal.* **2006**, *348*, 1391.

[5] a) T. H. Pham, B. K. Lee, J. Kim, C. H. Lee, *J. Taiwan Inst. Chem. Eng.* **2016**, *64*, 220; b) T. H. Pham, B. K. Lee, J. Kim, *J. Taiwan Inst. Chem. Eng.* **2016**, *66*, 239; c) S. Salehi, M. Anbia, A. H. Hosseiny, M. Sepehrian, *J. Mol. Struct.* **2018**, *1173*, 792; d) S. Bahraminia, M. Anbia, E. Koohsaryan, *Int. J. Hydrogen Energy* **2020**, *45*, 31027.

[6] a) S. M. Gomha, Z. A. Muhammad, H. M. Abdel-aziz, I. K. Matar, A. A. El-Sayed, *Green Chem. Lett. Rev.* **2020**, *13*, 6; b) G. L. Petri, V. Spanò, R. Spatola, R. Holl, M. V. Raimondi, P. Barraja, A. Montalbano, *Eur. J. Med. Chem.* **2020**, *208*, 112783; c) D. Choudhari, S. Salunke-Gawali, D. Chakravarty, S. R. Shaikh, D. N. Lande, S. P. Gejji, R. Gonnade, *New J. Chem.* **2020**, *44*, 6889; d) N. Perin, L. Hok, A. Beč, L. Persoons, E. Vanstreels, D. Daelemans, M. Hranjec, *Eur. J. Med. Chem.* **2020**, *211*, 113003; e) S. Eryılmaz, E. T. Çelikoğlu, Ö. İdil, E. İnkaya, Z. Kozak, E. Mısır, M. Gül, *Bioorg. Chem.* **2020**, *95*, 103476; f) J. Zhu, Y. Wu, L. Xu, J. Jin, *Curr. Comput.-Aided Drug Des.* **2020**, *16*, 17; g) S. Y. Wang, X. C. Shi, P. Laborda, *Eur. J. Med. Chem.* **2020**, *185*, 111847.

[7] a) S. N. Mokale, S. S. Shinde, R. D. Elgire, J. N. Sangshetti, D. B. Shinde, *Bioorg. Med. Chem. Lett.* **2010**, *20*, 4424; b) O. Alam, S. A. Khan, N. Siddiqui, W. Ahsan, S. P. Verma, S. J. Gilani, *Eur. J. Med. Chem.* **2010**, *45*, 5113; c) O. Sari, V. Roy, M. Métifiot, C. Marchand, Y. Pommier, S. Bourg, L. A. Agrofoglio, *Eur. J. Med. Chem.* **2015**, *104*, 127; d) O. C. Agbaje, O. O. Fadeyi, S. A. Fadeyi, L. E. Myles, C. O. Okoro, *Bioorg. Med. Chem. Lett.* **2011**, *21*, 989; e) J. Knapik, M. G. Gündüz, K. Chmiel, K. Jurkiewicz, M. Kurek, L. Tajber, M. Paluch, *Eur. J. Pharm. Sci.* **2020**, *141*, 105083; f) R. H. Tale, A. H. Rodge, G. D. Hatnapure, A. P. Keche, *Bioorg. Med. Chem. Lett.* **2011**, *21*, 4648.

[8] B. B. Snider, Z. Shi, *J. Organomet. Chem.* **1993**, *58*, 3828.

[9] a) C. Biginelli, *Gazz. Chim. Ital.* **1893**, *23*, 360; b) J. K. Joseph, S. L. Jain, B. Sain, *J. Mol. Catal. A: Chem.* **2006**, *247*, 99.

[10] a) N. Y. Fu, Y. F. Yuan, Z. Cao, S. W. Wang, J. T. Wang, C. Peppe, *Tetrahedron* **2002**, *58*, 4801; b) B. C. Ranu, A. Hajra, U. Jana, *J. Organomet. Chem.* **2000**, *65*, 6270; c) J. S. Yadav, B. V. S. Reddy, R. Srinivas, C. Venugopal, T. Ramalingam, *Synthesis* **2001**, *2001*, 1341; d) J. Lu, H. Ma, *Synlett* **2000**, *2000*, 63; e) U. B. More, *Asian J. Chem.* **2012**, *24*, 1906; f) V. N. Pathak, R. Gupta, B. Varshney, *Indian J. Chem., Sect. B: Org. Chem. Incl. Med. Chem.* **2008**, *47*, 434; g) J. Lu, Y. Bai, Z. Wang, B. Yang, H. Ma, *Tetrahedron Lett.* **2000**, *41*, 9075; h) R. Varala, M. M. Alam, S. R. Adapa, *Synlett* **2003**, *2003*, 67; i) E. H. Hu, D. R. Sidler, U. H. Dolling, *J. Organomet. Chem.* **1998**, *63*, 3454; j) S. Tu, F. Fang, C. Miao, H. Jiang, Y. Feng, D. Shi, X. Wang, *Tetrahedron Lett.* **2003**, *44*, 6153.

[11] a) F. K. Keter, J. Darkwa, *BioMetals* **2012**, *25*, 9; b) G. Thirunarayanan, K. G. Sekar, *J. Korean Chem. Soc.* **2013**, *57*, 599.

[12] S. Kumar, S. Bawa, S. Drabu, R. Kumar, H. Gupta, *Recent Pat. Anti-Infect. Drug Discovery* **2009**, *4*, 154.

[13] J. M. Alex, R. Kumar, *J. Enzyme Inhib. Med. Chem.* **2014**, *29*, 427.

[14] U. Bauer, B. J. Egner, I. Nilsson, M. Berghult, *Tetrahedron Lett.* **2000**, *41*, 2713.

[15] a) K. Sivakumar, A. Santhanam, M. Natarajan, D. Velauthapillai, B. Rangasamy, *Int. J. Appl. Ceram. Technol.* **2016**, *13*, 1182; b) O. S. Travkina, M. R. Agliullin, N. A. Filippova, A. N. Khazipova, I. G. Danilova, N. G. Grigor'Eva, B. I. Kutepov, *RSC Adv.* **2017**, *7*, 32581; c) W. Rongchapo, C. Keawkumay, N. Osakoo, K. Deekamwong, N. Chanlek, S. Prayoonpokarach, J. Wittayakun, *Adsorpt. Sci. Technol.* **2018**, *36*, 684; d) E. Liu, B. Sarkar, Z. Chen, R. Naidu, *Microporous Mesoporous Mater.* **2016**, *225*, 450; e) S. A. M. Hanim, N. A. N. N. Malek, Z. Ibrahim, *Vacuum* **2017**, *143*, 344.

[16] a) N. A. Liberto, S. de Paiva, Â. de Fátima, S. A. Fernandes, *Tetrahedron* **2013**, *69*, 8245; b) A. Rajack, K. Yuvaraju, C. Praveen, Y. L. N. Murthy, *J. Mol. Catal. A: Chem.* **2013**, *370*, 197; c) M. M. Heravi, K. Bakhtiari, F. F. Bamoharram, *Catal. Commun.* **2006**, *7*, 373; d) P. Salehi, M. Dabiri, M. A. Zolfigol, M. A. Bodaghi-Fard, *Tetrahedron Lett.* **2003**, *44*, 2889; e) A. Ghorbani-Choghamarani, P. Zamani, *Chin. Chem. Lett.* **2013**, *24*, 804; f) H. S. Chandak, N. P. Lad, P. P. Upare, *Catal. Lett.* **2009**, *131*, 469; g) R. V. Yarapathi, S. Kurva, S. Tammishetti, *Catal. Commun.* **2004**, *5*, 511; h) M. M. Heravi, F. Derikvand, F. F. Bamoharram, *J. Mol. Catal. A: Chem.* **2005**, *242*, 173; i) A. Maleki, P. Zand, Z. Mohseni, *ChemistrySelect* **2017**, *2*, 2740; j) M. Yadollahi, H. Hamadi, V. Nobakht, *Appl. Organomet. Chem.* **2019**, *33*, 4629.

[17] a) O. Mahé, D. Frath, I. Dez, F. Marsais, V. Levacher, J. F. Brière, *Org. Biomol. Chem.* **2009**, *7*, 3648; b) A. P. S. Bonakdar, A. Sadeghi, H. R. Aghaei, K. Beheshtimaal, S. M. R. Nazifi, A. R. Massah, *Russ. J. Bioorg. Chem.* **2020**, *46*, 371; c) J. Cao, J. Zang, C. Ma, X. Li, J. Hou, J. Li, Y. Zhang, *ChemMedChem* **2018**, *13*, 431; d) F. Özdemir Güney, İ. Ö. İlhan, S. Akkoç, *Synth. Commun.* **2019**, *49*, 2417; e) X. Bai, W. Q. Shi, H. F. Chen, P. Zhang, Y. Li, S. F. Yin, *Chem. Nat. Compd.* **2012**, *48*, 60; f) N. Raghav, M. Singh, *Bioorg. Med. Chem.* **2014**, *22*, 4233; g) G. Cocconcelli, E. Diodato, A. Caricasole, G. Gaviraghi, E. Genesio, C. Ghiron, G. C. Terstappen, *Bioorg. Med. Chem.* **2008**, *16*, 2043.

SUPPORTING INFORMATION

Additional supporting information may be found online in the Supporting Information section at the end of this article.

How to cite this article: R. Razavian Mofrad, H. Kabirifard, M. Tajbakhsh, G. Firouzzadeh Pasha, *Appl Organomet Chem* **2021**, e6383. https://doi.org/10.1002/aoc.6383